ELSEVIER

Materials Science and Engineering A 406 (2005) 268–273

MATERIALS SCIENCE & ENGINEERING A

www.elsevier.com/locate/msea

Developing high-pressure torsion for use with bulk samples

Genki Sakai [a], Katsuaki Nakamura [a], Zenji Horita [a], Terence G. Langdon [b,*]

[a] *Department of Materials Science and Engineering, Faculty of Engineering, Kyushu University, Fukuoka 812-8581, Japan*
[b] *Departments of Aerospace and Mechanical Engineering and Materials Science, University of Southern California, Los Angeles, CA 90089-1453, USA*

Received in revised form 16 June 2005; accepted 28 June 2005

Abstract

Experiments were conducted to examine the feasibility of extending conventional processing with high-pressure torsion (HPT) from use with thin disks with thickness of ∼1 mm to bulk cylindrical samples with height of ∼8 mm. Two cylindrical samples of an Al–Mg–Sc alloy were processed through 1/4 and 1 turn and then examined on different planes of sectioning. The results confirm the potential for using HPT with small cylinders but they show there are significant and systematic variations in the values of the Vickers microhardness throughout the samples after processing. After one turn in HPT, the highest values of the microhardness were achieved in the central plane around the outer edge of the sample where the hardness increased by a factor of >2 compared with the solution-treated condition. Microstructural examination revealed an array of equiaxed grains in this region with an average grain size of ∼200 nm.

Keywords: Hardness; High-pressure torsion; Severe plastic deformation; Microstructure; Ultrafine grains

1. Introduction

Considerable interest has developed recently in using severe plastic deformation (SPD) to process polycrystalline metals for the production of ultrafine-grained microstructures [1,2]. Typically, the grain sizes produced using SPD are in the submicrometer or nanometer range and thus they are smaller than the grain sizes achieved using conventional thermo-mechanical processing.

Several SPD processing techniques are now available but most interest has centered on the procedures of equal-channel angular pressing (ECAP) where a rod or bar is pressed repetitively through a die constrained within a channel bent through an abrupt angle [3–6] and high-pressure torsion (HPT) where a disk is subjected to a high pressure and concurrent torsional straining [7–9]. In general, it is easy to conduct ECAP processing and the technique may be readily scaled-up for the production of large bulk samples [10]. However, processing by HPT has two advantages over ECAP because it tends to produce both smaller grain sizes [11–14] and a higher fraction of boundaries having high angles of misorientation [12,14]. In addition, HPT processing may be used for the consolidation of fine particles [15,16] and amorphous ribbons [17].

A current major disadvantage of processing by HPT is that the specimen size is very small. Following the early work by Bridgman [18], where thin disks were compressed and strained in torsion to very large strains, the samples used for HPT have been consistently in the form of thin disks with diameters in the range of ∼10–20 mm and average thicknesses of ∼1 mm. This small size may be appropriate for the subsequent use of processed samples in electronic devices but it precludes the use of HPT processing for the production of materials for structural applications. Accordingly, the present investigation was initiated to provide a first evaluation of the potential for scaling-up the HPT process for use with bulk samples. Specifically, the present experiments were conducted using samples in a cylindrical form with a diameter of 10 mm and a height close to ∼8.5 mm. As will be demonstrated, HPT processing may be used with these larger samples but it was found that, at least after a single turn in torsion, the deformed microstructure is inhomogeneous with variations both across the central plane

* Corresponding author. Tel.: +1 213 740 0491; fax: +1 213 740 8071.
E-mail address: langdon@usc.edu (T.G. Langdon).

0921-5093/$ – see front matter © 2005 Elsevier B.V. All rights reserved.
doi:10.1016/j.msea.2005.06.049

of the sample and between the central and upper and lower sections.

2. Experimental material and procedures

An Al–3 wt.% Mg–0.2 wt.% Sc alloy was used for these experiments where this alloy was selected because the microstructure and properties are well documented after processing by ECAP [19–27] and HPT [28]. The alloy was prepared as an ingot using 99.99% purity aluminum, 99.9% purity magnesium and 99.999% purity scandium: the method of preparation was described earlier [23]. The ingot was homogenized in air at 753 K for 24 h, cut into a bar with dimensions of 18 mm × 18 mm × 160 mm, swaged into a rod with a diameter of 12 mm, lathed to a diameter of 10 mm and then cut into small cylinders with heights of 8.6 mm. These cylinders were solution treated in air for 5 h at 873 K to give an initial grain size of ∼0.5 mm. Following the solution treatment, the ends of the cylinders were lightly ground to give an initial height of 8.57 mm.

A special HPT facility was constructed for use in these experiments and this facility is illustrated schematically in Fig. 1. All parts of the facility were made from high-strength tool steel. The facility consisted of upper and lower anvils and three separate parts that were constructed in order to apply pressure and torsional straining to the sample. The central parts of the die consisted of cylindrical blocks that were mounted on the two anvils in exact alignment. Each of these blocks was surrounded by close-fitting cylindrical rings that were 4 mm longer than the central blocks and with the upper parts of the inner surfaces inclined outwards at an angle of 5° with the perpendicular. These cylindrical rings were surrounded by two additional rings, also made of tool steel, that were incorporated into the design as a safety measure to prevent an accident in the event that the inner die broke during straining. These outer rings are labeled the case in the illustration on the left in Fig. 1 and it is apparent from the illustration on the right, which shows the facility in operation

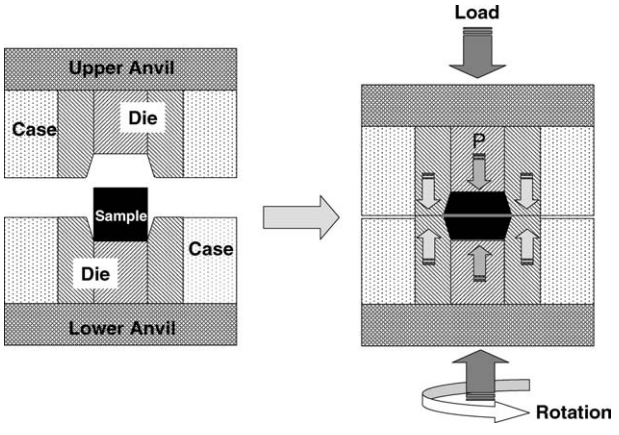

Fig. 1. Schematic illustration of the HPT facility (on left) and in operation with a pressure *P* (on right).

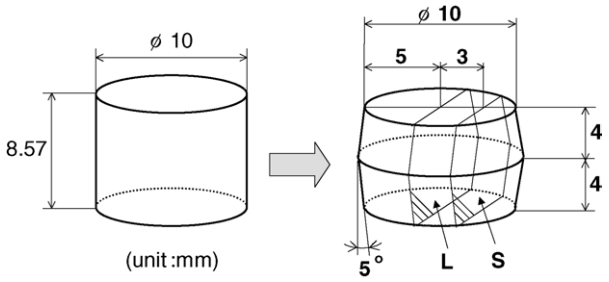

Fig. 2. Specimen shape initially (on left) and during HPT processing (on right): observations were undertaken on the two sectional planes labeled L and S.

with a pressure *P*, that the lower outer ring was constructed with a height approximately 1 mm shorter than the inner die to ensure that it experienced no pressure during the loading and straining operation. Since the confining die has edges inclined at 5° to the perpendicular, the specimen shape is changed from the initial configuration shown on the left in Fig. 2 to the final configuration shown on the right after application of the pressure *P*. Thus, the total height of the cylinder was reduced to 8 mm on application of the pressure and the specimen expanded outwards into a barrel-shaped configuration to fill the die. It is important to note that the total volume of the sample remained unchanged when it was forced into the barrel shape. In addition, there was a significant advantage in using this configuration because it was relatively easy to remove the sample from the die after testing.

During testing, the lower anvil was rotated with respect to the upper anvil at a rotation speed of 1 rpm. All testing was conducted at room temperature under an applied load of 9.3 tonnes, equivalent to an imposed pressure, *P*, of 1 GPa. In the present experiments, the torsional straining was terminated after either 1/4 or 1 turn, where, following the earlier proposal for conventional HPT, the strain is expressed solely in terms of the number of revolutions imposed on the sample, *N* [29].

Following HPT, the values of the Vickers microhardness, Hv, were recorded on a longitudinal section through the center of the cylinder labeled plane L on the right in Fig. 2. The values of Hv were recorded on this plane either in a rectilinear grid pattern or at discrete points having a spacing of 1 mm. Each separate value of Hv was determined by applying a load of 25 g for 20 s.

Microstructural observations were undertaken both on the longitudinal plane labeled L in Fig. 2 and on a secondary plane labeled S oriented parallel to plane L but displaced laterally from the center of the cylinder by 3 mm. These sections were mechanically polished to a mirror-like finish and then electro-polished in an aqueous solution of 5% HBF_4 for observations using optical microscopy. For transmission electron microscopy (TEM), samples were sliced to a thickness of ∼0.15 mm on plane S, disks were punched out with diameters of 3 mm, and these disks were mechanically polished and then electro-polished to perforation at room temperature

using a twin-jet polishing unit with a solution of 10% $HClO_4$, 20% $C_3H_8O_3$ and 70% C_2H_5OH. The perforated disks were examined using an Hitachi H-8100 microscope operating at 200 kV. Selected area electron diffraction (SAED) patterns were recorded from areas with diameters of 7.5 μm.

3. Experimental results

Figs. 3 and 4 show montages of the longitudinal plane L after totals of 1/4 or 1 turn, respectively, where the small diagrams at upper right indicate the plane of sectioning. The most significant characteristic of these sections is the clear evidence for flow patterns that delineate the flow of material towards the outer edges of the cylinder in the vicinity of the central section. For both conditions, but especially for the situation where $N = 1$ turn in Fig. 4, there are heavily deformed zones at the edges of the cylinders at the mid-section and within these zones the individual grain configurations are no longer visible. Outside of these heavily deformed regions, the grains tend to be elongated along the flow directions. It is apparent also that there are increases in both the thickness of the heavily deformed zones in a vertical sense and the width of these zones in a horizontal sense when the number of turns is increased from 1/4 to 1. For both experimental conditions, the grains appear to be less elongated near the middle of the central plane.

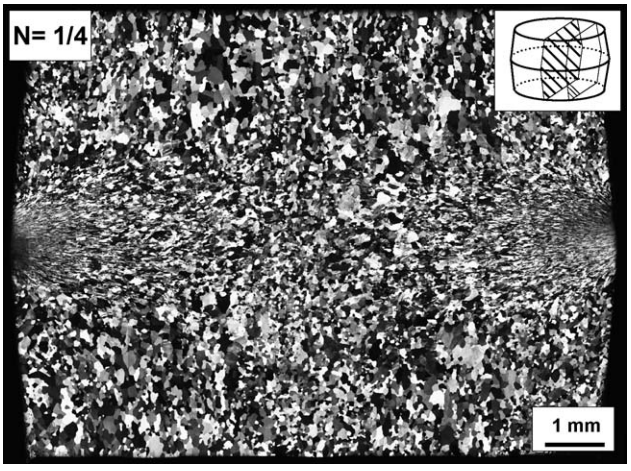

Fig. 3. Montage on the longitudinal plane L after $N = 1/4$ turn: the plane of sectioning is indicated at upper right.

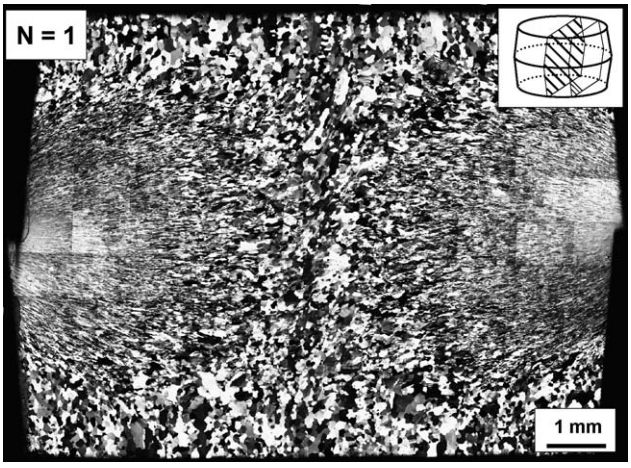

Fig. 4. Montage on the longitudinal plane L after $N = 1$ turn: the plane of sectioning is indicated at upper right.

The corresponding microhardness measurements are shown in Fig. 5, using a gray-scale representation for the condition where $N = 1$ turn, where the value of Hv within each 1 mm × 1 mm is represented pictorially using a scale factor of 20 for the individual values of Hv: the higher values of Hv are shown in a darker gray and the precise significance of the gray scale is depicted at the lower right. Inspection of Fig. 5 shows there are higher values of Hv in the vicinity of the outer edges at one-half of the height and the values of Hv decrease both towards the center of the cylinder and towards the upper and lower surfaces.

The variation of Hv across the horizontal mid-section of the cylinder is depicted in Fig. 6 where it is apparent that the hardness reaches maximum values of ∼140–150 at both of the outer edges but decreases to ∼95 at the center of the cylinder. The lower broken line in Fig. 6 delineates the solution treated condition where Hv ≈ 63. Thus, it is concluded that there is a measurable increase in hardness in the center of the cylinder after a single turn.

Fig. 7 shows a similar plot for the variation of Hv across vertical sections through the cylinder where the horizontal positions labeled from 0 to 5 correspond to the vertical sections indicated in Fig. 5 and position 0 is located at the central line. These lines confirm the high values of Hv that are achieved at the outer edges in the central region of the cylinder and the lower values of Hv at all other points.

Fig. 8 gives a montage of optical micrographs taken on plane S after 1 turn, where the plane of sectioning is again shown in the inset at upper right. The heavily deformed zones are again visible at the edges of the central section, the shapes

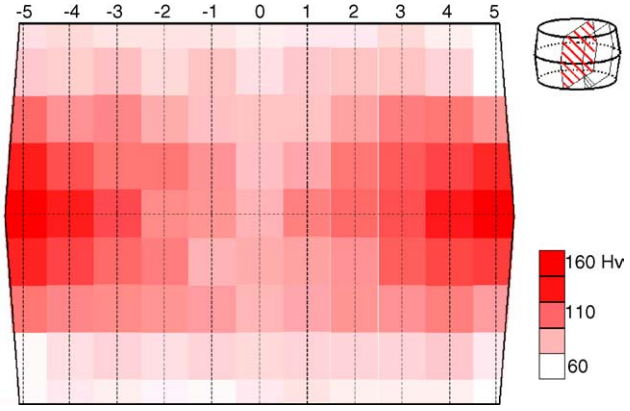

Fig. 5. Gray-scale representation of the Vickers microhardness on the L plane after $N = 1$ turn: the significance of the scale is indicated at lower right.

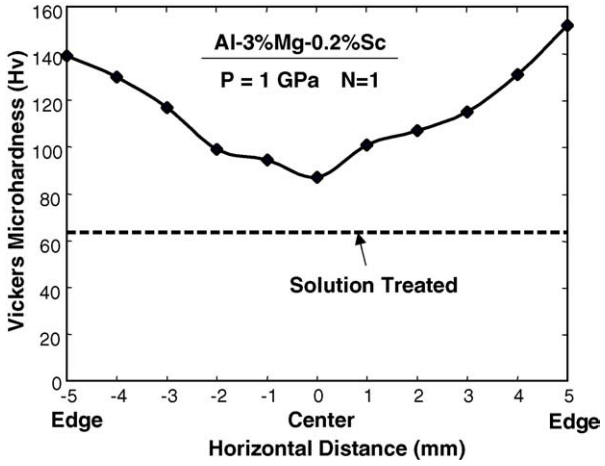

Fig. 6. Variation of Vickers microhardness across the horizontal mid-section of the cylinder: the lower broken line delineates the solution-treated condition.

of the grains indicate very intense flow and the alignments of the numerous grains provide a very clear delineation of the flow pattern associated with the torsional straining.

Representative TEM photomicrographs are shown in Fig. 9 for samples taken from plane S at (a) the center region of the sample labeled A in Fig. 8 and (b) an outer region near the edge of the specimen labeled B in Fig. 8. It is apparent that the microstructures in these two regions are different. In the outer region in Fig. 9(b), the grains are very fine and essentially equiaxed with an average grain size of ~0.2 μm. In this region the SAED pattern exhibits rings indicating the presence of a high fraction of boundaries having high angles of misorientation. By contrast, the grains are elongated in the central region in Fig. 9(a), there is a high dislocation density and the SAED pattern indicates that many of the boundaries have low angles of misorientation.

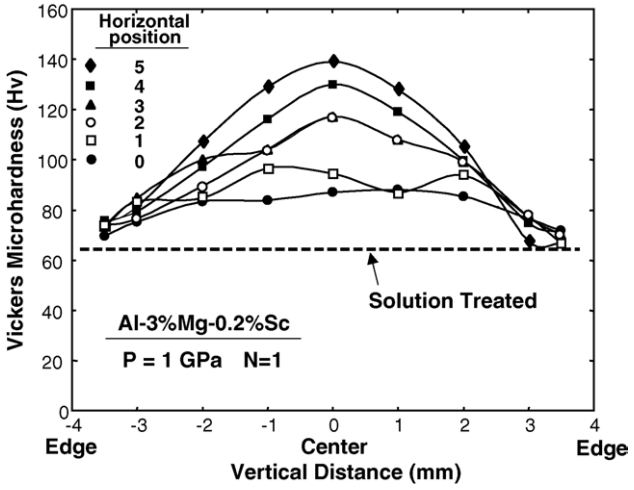

Fig. 7. Variation of Vickers microhardness across vertical sections of the cylinder where position 0 corresponds to the center line and the other positions are indicated in Fig. 5: the lower broken line delineates the solution-treated condition.

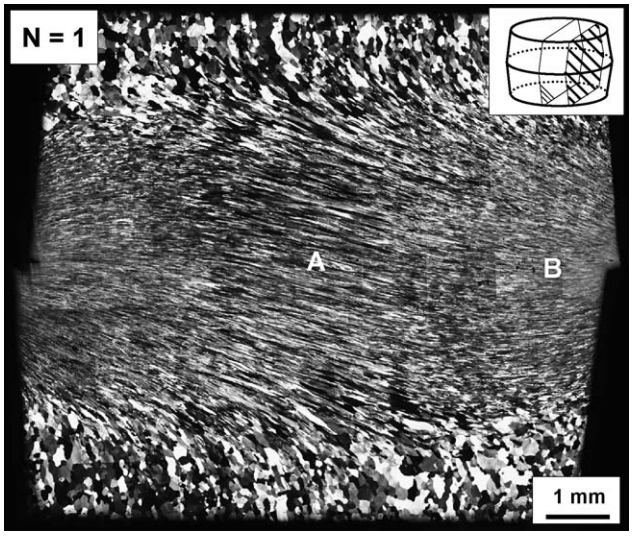

Fig. 8. Montage on the secondary plane S after $N = 1$ turn: the plane of sectioning is indicated at upper right.

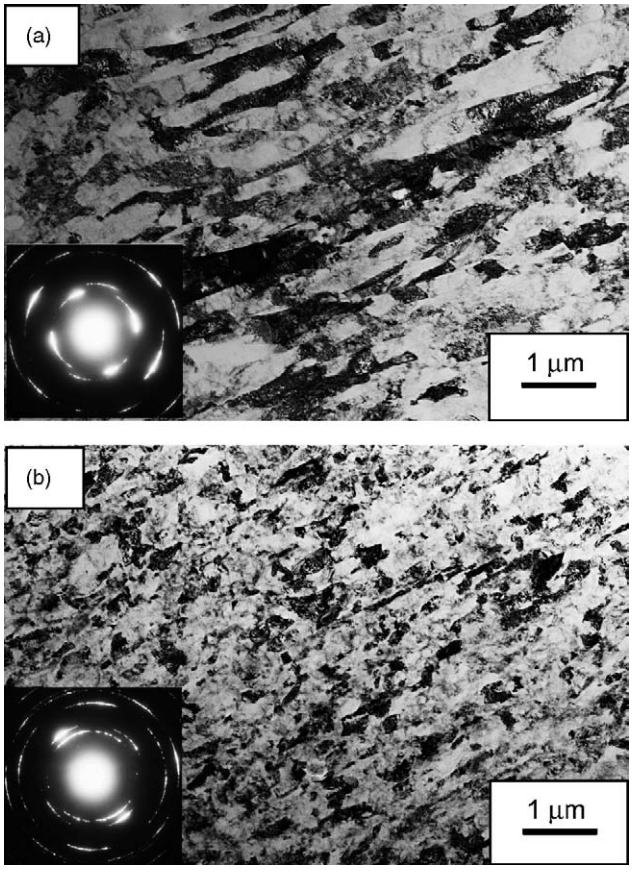

Fig. 9. Microstructures on the secondary plane S at (a) the center region and (b) an outer region, these positions are labeled A and B in Fig. 8.

4. Discussion

Processing by HPT is very attractive because there is a potential for producing exceptional grain refinement to the

nanometer level. However, HPT processing has the disadvantage that the conventional disk samples are extremely small with thicknesses of the order of ∼1 mm. The present investigation demonstrates the possibility of extending the HPT process to include the torsional straining of bulk samples in the form of small cylinders. In this research, HPT processing was applied to a cylinder of an Al–Mg–Sc alloy having a diameter of 10 mm and a height close to 8 mm. After a single turn of torsional straining the experimental results demonstrate the occurrence of substantial variations in the measured values of the Vickers microhardness both across the sample in a lateral plane at the mid-section and in vertical sections cut through the sample. Despite these variations, it is instructive to note that, in the central section in the vicinity of the outer edge of the sample, the hardness increased above the solution-treated value by a factor of >2 (Fig. 7) and the grain size was reduced from an initial value of ∼0.5 mm to an ultrafine value of ∼200 nm (Fig. 9(b)). This latter grain size is typical of the extremely small grain sizes achieved in conventional HPT with disk specimens [11–14].

It is now recognized that surface properties, such as wear-resistance, are often important in determining the useful life of an industrial component. This recognition has led to the development of numerous surface-modification techniques, such as friction stir welding and friction stir processing, in which significant grain refinement is achieved in a relatively thin surface region [30–34]. It is instructive to note, however, that these procedures generally produce less grain refinement than in HPT processing. For example, it was reported that friction stir processing gave mean spatial grain sizes of ∼1.5 μm in an Al–4% Mg–1% Zr alloy [33] and ∼3.3 μm in an Al-7075 alloy [30], whereas, the grain sizes achieved in Al-based alloys by HPT processing are generally of the order of ∼200–300 nm.

More detailed experiments are required to fully document the potential for achieving optimum microstructures and superior mechanical properties through the application of HPT processing to bulk solids. Nevertheless, these initial results demonstrate the feasibility of extending HPT to cylindrical specimens that are significantly larger than the conventional thin disks.

5. Summary and conclusions

1. A bulk sample of an Al–Mg–Sc alloy, in the form of a short cylinder with diameter of 10 mm and height of ∼8 mm, was successfully processed by high-pressure torsion through 1 turn.
2. After processing, there were significant but systematic variations in the values of the Vickers microhardess throughout the sample with the highest hardness values occurring around the edge of the sample in the central plane.
3. In the central plane in the vicinity of the outer edge, the hardness increased by a factor of >2 compared with the solution-treated condition and the grain size was reduced from an initial value of ∼0.5 mm to an as-processed value of ∼200 nm.

Acknowledgements

We thank Mr. Masuharu Ogawa for assistance with the construction of the bulk HPT facility and Mr. Yuichi Miyahara and Dr. Koji Neishi for assistance with the experiments. This work was supported in part by a Grant-in-Aid for Scientific Research from the Ministry of Education, Culture, Sports, Science and Technology of Japan, in part by the Light Metals Educational Foundation of Japan and in part by the National Science Foundation of the United States under Grant No. DMR-0243331.

References

[1] R.Z. Valiev, R.K. Islamgaliev, I.V. Alexandrov, Prog. Mater. Sci. 45 (2000) 103.
[2] M.J. Zehetbauer, R.Z. Valiev (Eds.), Nanomaterials by Severe Plastic Deformation: Fundamentals, Processing, Applications, Wiley/VCH, Weinheim/Germany, 2004.
[3] V.M. Segal, V.I. Reznikov, A.E. Drobyshevskiy, V.I. Kopylov, Russian Metall. 1 (1981) 99.
[4] Y. Iwahashi, Z. Horita, M. Nemoto, T.G. Langdon, Acta Mater. 45 (1997) 4733.
[5] Y. Iwahashi, Z. Horita, M. Nemoto, T.G. Langdon, Acta Mater. 46 (1998) 3317.
[6] M. Furukawa, Z. Horita, M. Nemoto, T.G. Langdon, J. Mater. Sci. 36 (2001) 2835.
[7] N.A. Smirnova, V.I. Levit, V.I. Pilyugin, R.I. Kuznetsov, L.S. Davydova, V.A. Sazonova, Fiz. Met. Metalloved. 68 (1986) 1170.
[8] A.P. Zhilyaev, S. Lee, G.V. Nurislamova, R.Z. Valiev, T.G. Langdon, Scripta Mater. 44 (2001) 2753.
[9] A.P. Zhilyaev, G.V. Nurislamova, B.-K. Kim, M.D. Baró, J.A. Szpunar, T.G. Langdon, Acta Mater. 51 (2003) 753.
[10] Z. Horita, T. Fujinami, T.G. Langdon, Mater. Sci. Eng. A 318 (2001) 34.
[11] V.V. Stolyarov, Y.T. Zhu, T.C. Lowe, R.K. Islamgaliev, R.Z. Valiev, Nanostruct. Mater. 11 (1999) 947.
[12] A.P. Zhilyaev, B.-K. Kim, G.V. Nurislamova, M.D. Baró, J.A. Szpunar, T.G. Langdon, Scripta Mater. 48 (2002) 575.
[13] V. Stolyarov, R.Z. Valiev, in: M.J. Zehetbauer, R.Z. Valiev (Eds.), Nanomaterials by Severe Plastic Deformation, Wiley/VCH, Weinheim/Germany, 2004, p. 125.
[14] A.P. Zhilyaev, B.-K. Kim, J.A. Szpunar, M.D. Baró, T.G. Langdon, Mater. Sci. Eng. A 391 (2005) 377.
[15] I.V. Alexandrov, Y.T. Zhu, T.C. Lowe, R.K. Islamgaliev, R.Z. Valiev, Nanostruct. Mater. 10 (1998) 45.
[16] A.R. Yavari, W.J. Botta Filho, C.A.D. Rodrigues, C. Cardoso, R.Z. Valiev, Scripta Mater. 46 (2002) 711.
[17] J. Sort, D.C. Ile, A.P. Zhilyaev, A. Concustell, T. Czeppe, M. Stoica, S. Suriñach, J. Eckert, M.D. Baró, Scripta Mater. 50 (2004) 1221.
[18] P.W. Bridgman, Studies in Large Plastic Flow and Fracture, McGraw-Hill, New York, 1952.
[19] S. Komura, P.B. Berbon, M. Furukawa, Z. Horita, M. Nemoto, T.G. Langdon, Scripta Mater. 38 (1998) 1851.
[20] P.B. Berbon, S. Komura, A. Utsunomiya, Z. Horita, M. Furukawa, M. Nemoto, T.G. Langdon, Mater. Trans. JIM 40 (1999) 772.

[21] Z. Horita, M. Furukawa, M. Nemoto, A.J. Barnes, T.G. Langdon, Acta Mater. 48 (2000) 3633.
[22] S. Komura, Z. Horita, M. Furukawa, M. Nemoto, T.G. Langdon, J. Mater. Res. 15 (2000) 2571.
[23] S. Komura, Z. Horita, M. Furukawa, M. Nemoto, T.G. Langdon, Metall. Mater. Trans. A 32A (2001) 707.
[24] M. Furukawa, A. Utsunomiya, K. Matsubara, Z. Horita, T.G. Langdon, Acta Mater. 49 (2001) 3829.
[25] S. Komura, M. Furukawa, Z. Horita, M. Nemoto, T.G. Langdon, Mater. Sci. Eng. A 297 (2001) 111.
[26] S. Lee, A. Utsunomiya, H. Akamatsu, K. Neishi, M. Furukawa, Z. Horita, T.G. Langdon, Acta Mater. 50 (2002) 553.
[27] G. Sakai, Z. Horita, T.G. Langdon, Mater. Trans. 45 (2004) 3079.
[28] G. Sakai, Z. Horita, T.G. Langdon, Mater. Sci. Eng. A 393 (2005) 344.
[29] R.Z. Valiev, Yu.V. Ivanisenko, E.F. Rauch, B. Baudelet, Acta Mater. 44 (1966) 4705.
[30] R.S. Mishra, M.W. Mahoney, S.X. McFadden, N.A. Mara, A.K. Mukherjee, Scripta Mater. 42 (2000) 163.
[31] R.S. Mishra, Adv. Mater. Proc. 16 (10) (2003) 43.
[32] R.S. Mishra, Z.Y. Ma, I. Charit, Mater. Sci. Eng. A 341 (2003) 307.
[33] Z.Y. Ma, R.S. Mishra, M.W. Mahoney, R. Grimes, Mater. Sci. Eng. A 351 (2003) 148.
[34] K. Oh-ishi, T.R. McNelley, Metall. Mater. Trans. A 35A (2004) 2951.